AN ALGEBRAIC MULTIGRID METHOD FOR LINEAR ELASTICITY

DANIEL OELTZ*

Abstract. We present an algebraic multigrid method for the solution of linear (block-)systems coming from a discretization of a system of partial differential equations. It generalizes the classical AMG approach for scalar problems to systems of PDEs in a natural blockwise fashion. We show that the block interpolation, described in this paper, reproduces the rigid body modes, i.e. the kernel elements of the linear elasticity operator. It is well known from geometric multigrid methods that this reproduction of the kernel elements is an essential property to obtain optimal convergence rates which are independent of the problem size. Finally the presentation of numerical experiments confirms that the method is robust and stable with fast convergence for a variety of discretized elasticity problems.

1. Introduction. The solution of large sparse linear systems is an essential ingredient in most scientific computations. The ever growing demand for efficient solvers led to the development of geometric multigrid methods in the 1970's [2, 3, 11, 12]. But for many applications it is very difficult to construct a sequence of (nested) discretizations or meshes needed for geometric multigrid. Furthermore, they are not robust w.r.t. deterioration of coefficients of the operator and singular perturbations. In the 1980's algebraic multigrid (AMG) methods were developed [4, 6, 7, 8, 14] to cope with these problems by extending the main ideas of geometric multigrid methods to a purely algebraic setting. The solver is based only on information available from the linear system to be solved. These methods can be applied successfully to many linear systems which come from a discretization of a scalar (elliptic) partial differential equation (PDE) [10, 9, 16]. But in the case of systems of PDEs most of the classical AMG methods fail.

In this paper we present a generalization of classical AMG to systems of PDEs where we assume only that the linear system is provided in point block form, i.e. all unknown coefficients corresponding to a node of the discretization make up local blocks of the system matrix. This approach was first proposed by Brandt [5]. Thereby, in a natural way, the restriction and prolongation operators can be defined in a blockwise fashion. We show in this paper that this leads to the the exact interpolation of the kernel elements of linear elasticity for a basic interpolation scheme and standard coarse grids in section 3. This is a theoretical justification of the so-called point-block approach. Furthermore, this main result shows that classic AMG can successfully be applied to the system case and no modifications as smoothed aggregation [17] or other techniques are really necessary to obtain fast convergence. We show the results of numerical experiments which also confirm our findings.

The remainder of the paper is organized as follows: First, we briefly discuss two issues why classical AMG can run into difficulties for systems. Then we describe our point-block generalization of classical AMG. It turns out that this approach overcomes these two difficulties. As a main result, we prove in section 3 the exact interpolation of the kernel elements of linear elasticity, called rigid body modes, which is, as for any multigrid algorithm, a fundamental property for the convergence behavior of the method. In section 4, we present numerical results of the method for discretizations from linear elasticity. We examine the stability of the method with respect to the

*Sonderforschungsbereich 408, Institut für Angewandte Mathematik, Universität Bonn, Wegelerstr. 6, D-53115 Bonn, oeltz@iam.uni-bonn.de

mesh width and the robustness with respect to the Poisson ratio ν. At the end of the numerical section we present results for complex geometries and unstructured grids. Finally we conclude with some remarks in section 5.

2. Algebraic Multigrid for Systems of PDEs. Although classical AMG methods [4, 6, 7, 8, 14] lead to fast convergence for most discretizations of elliptic scalar PDEs, these methods converge very slowly in the system case. There are two main reasons for the deterioration of the convergence:

First, let us assume that all physical unknowns u_i, $i = 1, ..., d$, are discretized on the same grid $\Omega_h := \{x_i \mid x_i \in \mathbb{R}^d, i = 1, ..., n\}$. Then, different unknowns of the discretization belong to the same geometric grid point x_i. Classical AMG methods treat all unknowns as different geometric grid points. Therefore, the coarsening can lead to different geometric grids for different physical unknowns, which is in general not optimal and influences the convergence. A second problem is the accuracy of the interpolation schemes of classical AMG methods. Important for the convergence of any multigrid algorithm is the exact interpolation of the kernel elements of the continuous operator. While in the scalar case the kernel elements are most often only constant functions, which are interpolated exactly by classic interpolation formulas, the kernel in the case of a system is in general more complicated and standard interpolation schemes are not able to reproduce all kernel functions in the system case.

To solve these problems, we propose the so-called point-block approach which was first suggested in [5]. Here, we assume that all physical unknowns u_i are discretized on the same grid Ω_h. Let the discretized system be given in the following form:

$$\begin{pmatrix} A_{11} & A_{12} & \cdots & A_{1n} \\ A_{21} & A_{22} & \cdots & A_{2n} \\ \vdots & \ddots & \vdots & \vdots \\ A_{n1} & A_{n2} & \cdots & A_{nn} \end{pmatrix} \begin{pmatrix} \tilde{u}_1 \\ \tilde{u}_2 \\ \vdots \\ \tilde{u}_n \end{pmatrix} = \begin{pmatrix} \tilde{f}_1 \\ \tilde{f}_2 \\ \vdots \\ \tilde{f}_n \end{pmatrix}, \tag{2.1}$$

where $\tilde{u}_j \in \mathbb{R}^d$ are the components associated with the basis functions of the d different physical unknowns u_i on the grid point x_j.

Now, the generalization of classical scalar AMG methods to the block structure is straightforward. We simply use block-iteration schemes as smoothers, e.g the block Gauß–Seidel or block Jacobi smoothers. Furthermore, we generalize AMG-interpolation schemes to the block structure of the matrix A. Coarse grid selection is done by selecting coarse grid blocks and the appropriate unknowns as coarse grid unknowns. For the classic AMG approach of Ruge and Stüben we describe the details in the next subsection. It is obvious that the resulting coarse grids are the same for all unknown functions. Furthermore, we can show that the generalization of the interpolation to the block structure leads to exact interpolation of the kernel elements of the continuous operator for standard coarse grids, see section 3.

2.1. The point-block approach for the classic Ruge and Stüben AMG. Now we discuss the generalization of the basic Ruge and Stüben AMG [14] for the point-block approach. In our notation we mainly follow [16].

Fundamental to the coarse grid selection in AMG is the notion of strong couplings, which were originally defined among scalar unknowns (or grid points). Now we need a definition which is applicable to point blocks and hence gives a measure for the connectivity between grid points, again. To this end, we condense the block matrix A to a scalar matrix $\tilde{A}$ and apply the usual definition of strong couplings to the new matrix $\tilde{A}$. For the condensation we substitute for a fixed matrix norm $|||\cdot|||$ all block-entries by their norm. Hence we get the matrix $\tilde{A} = (a_{ij})$ with $a_{ij} = |||A_{ij}|||$. Then, according to the classic definition with fixed $0 \leq \alpha \leq 1$, we call a grid point i strongly coupled with j if $\tilde{a}_{ij} \geq \alpha \cdot \max_i \tilde{a}_{ij}$. We chose the row sum norm, which is easy to calculate and provides good results in our experiments. With the definition of strong couplings, we apply exactly the coarsening algorithm from the Ruge and Stüben AMG with the setup phase one and two [9].

In our code we use two generalizations of the so-called standard interpolation from [16]. Therefore we briefly describe this scalar interpolation method for a scalar matrix $A = (a_{ij})$. Let $N := \{1, ..., n\}$ be the index set of the grid Ω_h and $N_i := N \setminus \{i\}$. Let $S_i := \{j \mid i \text{ is strongly coupled to } j\}$ be the set of all blocks coupled to the block i, $C \subset N$ be the set of all coarse grid points and $F = N \setminus C$ the set of the fine grid points. The usual starting point for the standard interpolation is the direct interpolation. This interpolation is based on the characterization $Ae \approx 0$ for algebraically smooth error e and leads to the approximate equation

$$e_i = -\sum_{j \in N_i} a_{ij} e_j / a_{ii}, \tag{2.2}$$

where $i \in F$ denotes a fine grid point. Now, we define the set of interpolation points P_i for the fine grid point i as $P_i := C \cap S_i$. With this formula we obtain the interpolation formula of the direct interpolation

$$(Ie)_i = -\frac{(\sum_{j \in N_i} a_{ij})}{a_{ii} \cdot \sum_{j \in P_i} a_{ij}} \sum_{j \in P_i} a_{ij} e_j. \tag{2.3}$$

Here, the additional factor $(\sum_{j \in N} a_{ij})(a_{ii} \sum_{j \in P_i} a_{ij})^{-1}$ assures that constant vectors, which normally represent the constant functions, are interpolated exactly. As described in [16] the size and structure of the set P_i has a significant influence on the quality of interpolation and on the speed of convergence. Hence, for many problems, it is necessary to enlarge this set. Therefore we replace for a given fine grid point i every unknown coefficient e_j, $j \in S_i \cap F$, in (2.2) by the respective equation (2.2) for this point j. Thus we get the following new equation for i

$$e_i = -1/\hat{a}_{ii} \sum_{j \in N_i} \hat{a}_{ij} e_j, \tag{2.4}$$

where $\hat{a}_{ij} := a_{ij} - \sum_{k \in S_i \cap F} a_{ik} \cdot a_{kj} / a_{kk}$. Applying the direct interpolation to this modification (2.4) of (2.2) with the set of interpolation variables $\hat{P}_i := P_i \cup \bigcup_{j \in S_i \cap F} P_j$, where P_i is the previously defined set for the direct interpolation, we get another interpolation formula, which is traditionally called the standard interpolation, see [16].

There are two different possibilities for the generalization of the scalar interpolation formulas to the block matrix $A = (A_{ij})$, $A_{ij} \in \mathbb{R}^d$. First, we take the complete matrix blocks A_{ij} instead of the matrix entries a_{ij} and use them in the previous interpolation formulas. Analogously to the direct interpolation (2.3) we get what we call the block direct interpolation:

$$(Ie)_i = -A_{ii}^{-1} \left(\sum_{j \in N_i} A_{ij} \right) \left(\sum_{j \in P_i} A_{ij} \right)^{-1} \sum_{j \in P_i} A_{ij} e_j. \tag{2.5}$$

If we use for e_j, $j \in S_i \cap F$, similar to (2.2) the identity

$$e_j = -A_{jj}^{-1} \sum_{k \in N_j} A_{jk} e_k,$$

we get

$$e_i = -\hat{A}_{ii}^{-1} \sum_{j \in N_i} \hat{A}_{ij} e_j \tag{2.6}$$

with $\hat{A}_{ij} := A_{ij} - \sum_{k \in S_i \cap F} A_{kk}^{-1} A_{ik} \cdot A_{kj}$. Now we can, analogously to the previously discussed scalar case, apply the block direct interpolation to the new approximate equation (2.6) and get the block standard interpolation (BI). A second possibility to generalize the interpolation from the scalar to the system case, is to neglect the couplings between different physical unknowns. We achieve this by using the diagonals $D_{ij} = \mathrm{diag}(A_{ij})$ instead of the full blocks A_{ij} in the interpolation formulas. This leads to the so-called point standard interpolation (PI).

In the next section we show that the generalization of the block direct interpolation leads to the exact interpolation of the kernel elements of the operator from linear elasticity.

3. Interpolation of the rigid body modes. In linear elasticity we are looking for a displacement vector u of a solid described by the domain $\Omega \subset \mathbb{R}^{\{3,2\}}$ under the influence of an external force f and a surface force g, where $\Gamma_0 \subset \Omega$ is the part of the boundary under the influence of g and Γ_1 is the fixed part of the boundary. Let $\varepsilon(u) := (\varepsilon_{ij})_{i,j=1}^{3}$ be defined as $\varepsilon_{ij} := \frac{1}{2}(\partial_i u_j + \partial_j u_i)$, called the strain tensor. The bilinear form of the weak formulation of the problem is $a(u,v) := \int_\Omega \varepsilon(u) : \sigma(v) dx$, where σ can be described by

$$\begin{bmatrix} \sigma_{11} \\ \sigma_{22} \\ \sigma_{33} \\ \sigma_{12} \\ \sigma_{13} \\ \sigma_{23} \end{bmatrix} = \theta \cdot \begin{bmatrix} 1-\nu & \nu & \nu & 0 & 0 & 0 \\ \nu & 1-\nu & \nu & 0 & 0 & 0 \\ \nu & \nu & 1-\nu & 0 & 0 & 0 \\ 0 & 0 & 0 & 1-2\nu & 0 & 0 \\ 0 & 0 & 0 & 0 & 1-2\nu & 0 \\ 0 & 0 & 0 & 0 & 0 & 1-2\nu \end{bmatrix} \begin{bmatrix} \varepsilon_{11} \\ \varepsilon_{22} \\ \varepsilon_{33} \\ \varepsilon_{12} \\ \varepsilon_{13} \\ \varepsilon_{23} \end{bmatrix},$$

with $\theta := \frac{E}{(1+\nu)(1-2\nu)}$, $\frac{1}{2} > \nu > 0$ and E denotes the Young module. For the three-dimensional problem, the kernel elements of the operator consists of the elements

$$\varphi(x) = a \wedge x + b,$$

with fixed $a, b \in \mathbb{R}^3$. In the case of two dimensions, the kernel is spanned by the elements

$$\begin{pmatrix} 1 \\ 0 \end{pmatrix}, \begin{pmatrix} 0 \\ 1 \end{pmatrix}, \begin{pmatrix} x_2 \\ -x_1 \end{pmatrix}.$$

Now we consider the properties of the block direct interpolation on special grids. It will turn out that the rigid body modes are exactly reproduced. In the following we denote by φ_k^i, $1 \le k \le n$, $1 \le i \le d$, $d = 2, 3$ the nodal basis function for the grid point k with the i-th component being nonzero. We define $\Omega_{ij} := supp(\varphi_i^1) \cap supp(\varphi_j^1)$ We call the coarse grid point symmetric at the fine grid point $i \in F$, if for every coarse grid point $j \in C_i$ there is another coarse grid point $k \in C_i$, $k \neq j$, so that with a suitable $c \in \mathbb{R}^d$ and $q \in \mathbb{R}_+$ the mapping $Q(x) := -q \cdot x$ is a bijection between $\Omega_{ki} - \{x_i\}$ and $\Omega_{ji} - \{x_i\}$,

LEMMA 3.1. *Let $\Omega_h = \{1, ..., n\}$ be a grid and $\Omega_H \subset \Omega_h$ be the grid of coarse grid points. Let $\tilde{r} = (\tilde{r}_i)_{i=1}^n \in \mathbb{R}^{d \cdot n}$ be the coefficient vector for a rigid body mode $\tilde{r}$. Let the coarse grid be point symmetric at the fine grid point $i \in F$. Then, the block direct interpolation (2.5) interpolates $\tilde{r}_i$ exactly, i.e.*

$$(I\tilde{r})_i = \tilde{r}_i.$$

Proof. A straightforward computation shows the result for the constant functions. Therefore we only prove the result for the rotation $r(x) = (-x_2, x_1, 0)^T$. The coefficient vector for the representation in the nodal basis is then given by $\tilde{r} = (\tilde{r}_k)_{k=1}^n = ((-(x_k)_2, (x_k)_1, 0)^T)_{k=1}^n$ with $x_k \in \Omega_h$. For the fine grid point i we get

$$\begin{aligned}(I\tilde{r})_i &= -A_{ii}^{-1}(\sum_{j \in N} A_{ij})(\sum_{j \in P_i} A_{ij})^{-1} \sum_{j \in P_i} A_{ij}\tilde{r}_j \\ &= -A_{ii}^{-1}(\sum_{j \in N} A_{ij})(\sum_{j \in P_i} A_{ij})^{-1} \sum_{j \in P_i} A_{ij}(\tilde{r}_i + \tilde{r}_j - \tilde{r}_i).\end{aligned}$$

Since constant functions are interpolated exactly, we get

$$(I\tilde{r})_i = \tilde{r}_i - A_{ii}^{-1}(\sum_{j \in N} A_{ij})(\sum_{j \in P_i} A_{ij})^{-1} \sum_{j \in P_i} A_{ij}(\tilde{r}_j - \tilde{r}_i).$$

Therefore it suffices to show that the second sum is zero. With the above definition, the second sum is

$$-A_{ii}^{-1}(\sum_{j \in N} A_{ij})(\sum_{j \in P_i} A_{ij})^{-1} \sum_{j \in P_i} \begin{pmatrix} a(\varphi_i^1, r) \mid_{\Omega_{ij} - \{x_i\}} \\ a(\varphi_i^2, r) \mid_{\Omega_{ij} - \{x_i\}} \\ a(\varphi_i^3, r) \mid_{\Omega_{ij} - \{x_i\}} \end{pmatrix}.$$

Now we split the set P_i of interpolation points into two disjoint subsets $P_i = P_i^1 \cup P_i^2$ so that for every $k \in P_i^1$ it exists $\pi(k) \in P_i^2$ and a $q \in \mathbb{R}_+$ with $Q(x) := -q \cdot x$ is a bijective mapping from $\Omega_{ik} - \{x_i\}$ onto $\Omega_{i\pi(k)} - \{x_i\}$. Then it remains to show that

$$\begin{pmatrix} a(\varphi_i^1, r) \mid_{\Omega_{ij} - \{x_i\}} \\ a(\varphi_i^2, r) \mid_{\Omega_{ij} - \{x_i\}} \\ a(\varphi_i^3, r) \mid_{\Omega_{ij} - \{x_i\}} \end{pmatrix} = - \begin{pmatrix} a(\varphi_i^1, r) \mid_{\Omega_{i\pi(j)} - \{x_i\}} \\ a(\varphi_i^2, r) \mid_{\Omega_{i\pi(j)} - \{x_i\}} \\ a(\varphi_i^3, r) \mid_{\Omega_{i\pi(j)} - \{x_i\}} \end{pmatrix}. \tag{3.1}$$

Taking into account that $-q \cdot r(-q^{-1}x) = r(x)$ and using the transformation rule of integration, the equality (3.1) follows. □

As known from geometric multigrid methods, the exact reproduction of the kernel elements by the interpolation scheme is important for the convergence of the method to be independent of the problem size. Therefore this result is a theoretical justification for the approach in the case of discretized linear elasticity problems. It shows that the simple generalization of classic interpolation schemes to the block structure can lead to higher interpolation accuracy, so that also the second problem which leads to deterioration the deterioration of convergence of classical AMG in the case of systems of PDEs is solved. Therefore it can be expected, and this is validated in the next section, that in the system case the point-block AMG works as well as classical AMG in the case of scalar problems.

4. Numerical Results. In this section we present numerical results for the point standard- and the block standard interpolation from subsection 2.1. We set the right hand side to zero and start the iteration with a random start value normed to one in the L_2-norm. We stop the AMG-iteration when the residue in the L_2-norm was less then 10^{-12} and measure the speed of convergence by the asymptotic error reduction ρ, that is

$$\rho := \left(\frac{||e_k||_E}{||e_{k-10}||_E} \right)^{1/10}.$$

Here, e_j is the remaining error from the j-th iteration step and k is the number of the iteration step when the stopping criterion was reached. To give insight to the structure of the coarsening process and the coarser grids, we give the total-grid-complexity $c(G)$ and the total-operator-complexity $c(A)$, which are defined as

$$c(G) := \textstyle\sum_{i=0}^{J} n_u^i / n_u^0, \quad c(A) := \sum_{i=0}^{J} n_z^i / n_z^0,$$

where n_u^i is the number of unknowns and n_z^i the number of nonzero blocks of the i-th level, and $J+1$ is the total number of the levels. To minimize computational cost, it can be useful to delete small values from the prolongation matrix [16]. We compare the size of the matrix entries of one row of the condensed matrix $\tilde{I} = (\tilde{i}_{jk})$, which we get in the same way as $\tilde{A}$ for the calculation of the strong couplings by substituting every block P_{ij} by its operator norm $|||P_{ij}|||$. Then we delete a block entry I_{jk} if $\tilde{i}_{jk} < \alpha_{tr} \cdot \max_l \tilde{i}_{jl}$ is satisfied for a given fixed threshold α_{tr}. If not stated otherwise, we use the truncation parameter $\alpha_{tr} = 0.2$ and the setup parameter $\alpha = 0.25$. In the classic Ruge and Stüben AMG we need for the second setup phase an additional parameter β, which we set to $\beta = 0.35$. The operator on the coarsest level consists of only one block.

We give numerical results for different discretized linear elasticity problems in two and three dimensions. The discretizations were computed with the freely available program TOCHNOG [15]. If not stated otherwise, we use bilinear isoparametric elements with Lobatto integration.

First we show the asymptotic convergence behavior of the method to the problem size h which indicates convergence independent of the problem size. Then we examine convergence in the case of bad aspect ratios, where the method behaves as the classic Ruge and Stüben AMG in the case of anisotropic diffusion problems. Finally we give results for some complicated geometries and unstructured grids.

Example 1 (h-stability and robustness with respect to the Poisson ratio). In the first example we show the independence of the rate of convergence from the mesh width h of the discretization for a elasticity problem with Dirichlet boundary conditions on the unit square (the cube in three dimensions) with Poisson ratio $\nu = 0.3$. Then we show the robustness of the method for the two-dimensional problem with respect to the Poisson ration ν. The asymptotic error reduction ρ, the total-grid-complexity and the total-operator-complexity for the two-dimensional problem for different mesh widths are displayed in Table 4.1. Here, the Poisson ratio ν is 0.3. Both interpolations seem to result in convergence rates bounded uniformly away from one independent of the mesh width. The point standard interpolation provides faster convergence than the block standard interpolation. For example, the asymptotic error reduction of the point standard interpolation is $\rho = 0.26$ for $h = 1/256$ whereas the block standard interpolation obtains $\rho = 0.46$.

TABLE 4.1
Asymptotic error reduction and complexities for the two-dimensional Dirichlet-problem on the unit square in the case of the point standard interpolation (PI) and the block standard Interpolation (BI).

	PI			BI		
h	c(G)	c(A)	ρ	c(G)	c(A)	ρ
16	1.72	2.49	0.15	1.73	2.51	0.14
32	1.69	2.61	0.21	1.70	2.65	0.21
64	1.68	2.69	0.22	1.68	2.72	0.33
128	1.68	2.75	0.23	1.67	2.78	0.43
256	1.67	2.75	0.26	1.67	2.78	0.46

TABLE 4.2
Asymptotic error reduction and complexities for the three-dimensional Dirichlet-problem on the unit cube for the point standard interpolation (PI) and the block standard interpolation (BI).

	PI			BI		
h	c(G)	c(A)	ρ	c(G)	c(A)	ρ
16	1.64	3.25	0.18	1.65	3.64	0.16
32	1.62	3.44	0.27	1.62	3.97	0.26

In three dimensions, both interpolation schemes lead to similar results. For the mesh width $h = 1/32$ the method provides convergence rates of about $\rho = 0.26$ which are comparable to the two-dimensional case. Different to the two-dimensional problem is the operator-complexity, which is somewhat higher than in two dimensions. We have $c(A) = 3.97$ for the block standard interpolation with $h = 1/32$. This increase of $c(A)$ is independent of the choice of α_{tr} [13].

Since in practice the size of the Poisson ratio can vary substantially, the robustness of the method with respect to the Poisson ratio is an important property. Therefore we show in the left part of Figure 4.1 convergence results for a mesh width $h = 1/128$ and different Poisson ratios. For the point standard interpolation, up to the ratio $\nu \approx 0.36$ the speed of convergence declines very slowly to $\rho \approx 0.35$, while from that time on, convergence deteriorates substantially. In the case of the block standard interpolation, the convergence declines from the beginning. But qualitatively, there is a similar behavior as for the point standard interpolation: With growing ν, the deterioration becomes faster and faster. Nevertheless, the results are satisfactory for Poisson ratios $\nu \leq 0.4$, which are in practice the most important cases. The reason for the deterioration of convergence is of course the condition of the problem, which becomes worse with growing ν and is well known as Poisson locking [1]. For comparison with the results of other methods it should be noticed that we measure the reduction of the error and not the reduction of the residuum. The figures for the reduction of the residuum are much better than for the reduction of the error. For example for $\nu = 0.4$ and the point standard interpolation, we get an asymptotic error reduction $\rho \approx 0.66$ whereas the residue reduction is 0.51.

Example 2 (The cantilever beam). In the following example we focus on the problem of *bad aspect ratios*. We discretize the elasticity problem in two dimensions on a rectangular domain with the mesh width $h_{x_2} = l \cdot h_{x_1}$ where $l > 0$ is the relative length of the rectangle as shown in the left picture of Figure 4.2. In three dimensions we distinguish two cases:

$$\Omega = [0, l] \times [0, 1]^2 \text{ and } h_{x_1} = l \cdot h_{x_2} (= h_{x_3}), \tag{4.1}$$

$$\Omega = [0, l]^2 \times [0, 1] \text{ and } h_{x_1} = h_{x_2} = l \cdot h_{x_3}, \tag{4.2}$$

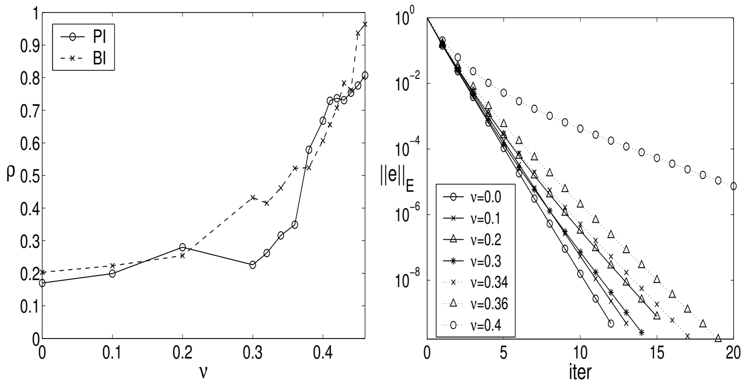

FIGURE 4.1. *Left: Asymptotic error reduction for the two-dimensional problems with $h = 1/128$ and varying Poisson ratios. Right: Convergence histories for the point standard interpolation and different Poisson ratios.*

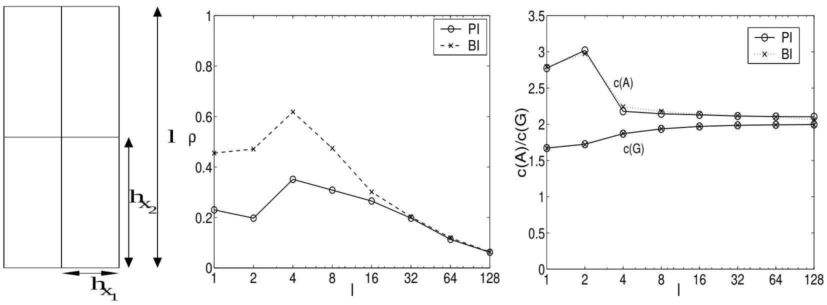

FIGURE 4.2. *Setting of the two-dimensional problem (left) of the cantilever beam. Asymptotic error reduction for different l (middle) and grid- and operator-complexities (right) for $h = 1/256$ and the point- (PI) and block standard interpolation (BI).*

as presented in Figure 4.3 (left).

In the two-dimensional case we expect similar results as for classical methods in the case of anisotropic diffusion: The more the rectangular is stretched, the more AMG behaves like a direct solver [9]. Indeed, looking at Figure 4.2, where convergence and complexity results for the two-dimensional problem with $h = 1/256$ are depicted, we find the expected behavior of the method. After a short decline of the speed of convergence until $l = 4$, independent of the applied interpolation, the convergence results are getting better, and we have at least an asymptotic error reduction rate $\rho = 0.06$ for both interpolations for the length $l = 128$. At the same time, we notice a deterioration of the total-operator-complexity. While for $l = 1$ the block standard interpolation leads to a complexity of $c(A) = 2.80$, the total-operator-complexity converges to the total-grid-complexity and reaches at the end the value $c(G) = 2.061$. This behavior relies on the semi-coarsening of the method, which can also be noticed for scalar anisotropic diffusion.

In the three-dimensional case, we have to distinguish between the two different domains. In case of the first domain (4.1), where the rectangular domain is just stretched in the x_1-direction, semi-coarsening is done in one direction only which does not influence the convergence result but the total-operator-complexity. This fact becomes clear in Figure 4.3 (top), which displays the results for $h = 1/32$. While

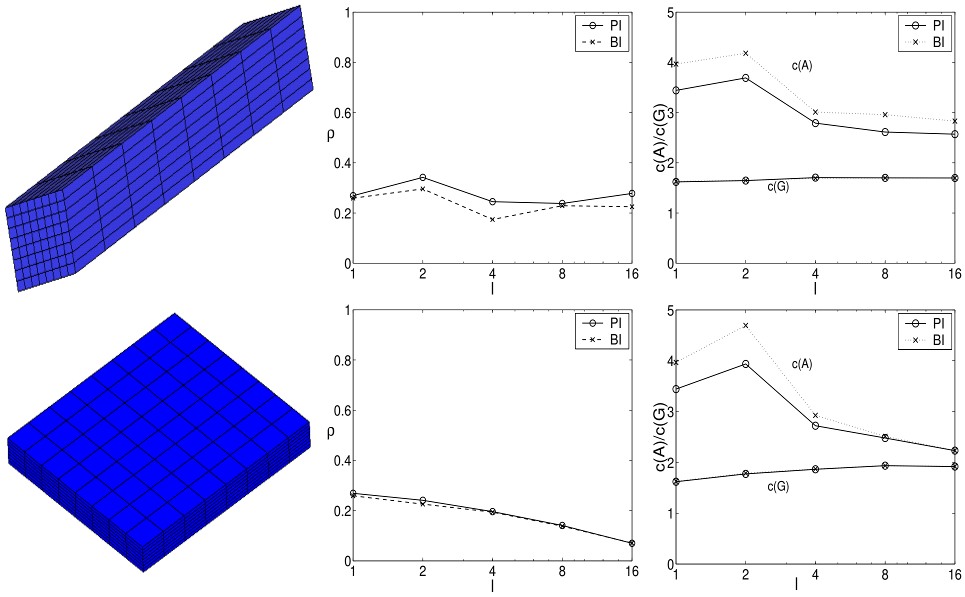

FIGURE 4.3. *Above: Convergence and complexity results for the first three dimensional problem 4.1 with $h = 1/32$. Bottom: convergence results for the second three dimensional problem 4.2 with $h = 1/32$. PI stands for the point standard interpolation and BI for the block standard interpolation.*

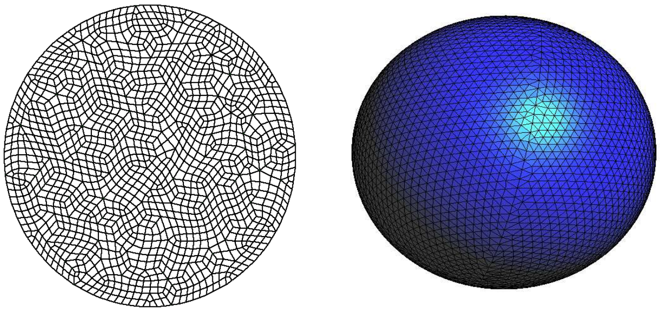

FIGURE 4.4. *The circle (left) and the sphere with the mesh.*

the asymptotic error reduction seems to be relatively independent ($\rho \approx 0.24$ with the worst result $\rho = 0.34$ for $l = 2$) of the parameter l, the total-operator-complexity falls from $c(A) = 3.44$ for $l = 1$ to $c(A) = 2.57$ for $l = 16$. For the second domain (4.2) the elasticity problem degenerates with growing l to a decoupled one-dimensional problem. Thus, the asymptotic error reduction and the total-operator-complexity decline for growing l. So, the method converges with $\rho = 0.070$ for $l = 16$ more than three times faster than in the case of $l = 1$ with $\rho = 0.27$.

Example 3 (Unstructured and complicated grids).

Now we consider problems with complicated geometries and unstructured grids, one of the cases AMG was developed for. In the first example, the elasticity equations in two dimensions are discretized on a circle with bilinear elements whereas the three-dimensional problem is discretized on the sphere with linear elements as shown in Figure 4.4. In the previous experiments the point standard interpolation led to

TABLE 4.3
Results of the two-dimensional problem on the circle for different problem sizes n and $\alpha = 0.25$ using point standard interpolation.

	$\omega = 1.0$			$\omega = 1.5$				
n	1/1	2/1	2/2	1/1	2/1	2/2	c(A)	c(G)
2342	0.37	0.33	0.30	0.26	0.16	0.14	2.85	1.70
9978	0.46	0.42	0.40	0.30	0.29	0.24	2.91	1.73
22594	0.44	0.42	0.39	0.35	0.28	0.27	3.12	1.73
90422	0.48	0.45	0.43	0.31	0.33	0.33	3.16	1.73

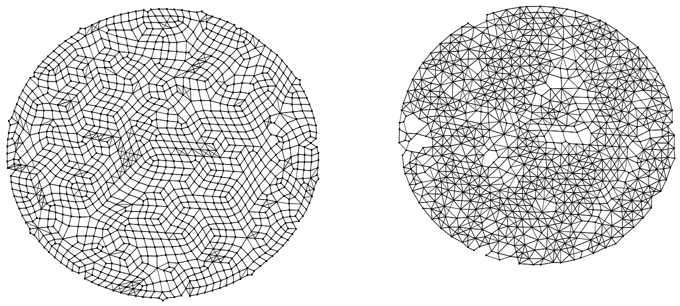

FIGURE 4.5. *Top: complete hierarchy of coarse grids (left) and first and second coarse grid (right). Middle: Fine grid (left) and first coarse grid (right) with strong couplings.*

convergence results better than or equal to the block standard interpolation. Hence we give in the following only the results for the point standard interpolation. Since for some problems the use of Block-SOR instead of Block-Gauß–Seidel [13] as a smoother can substantially improve the results, we give figures for the relaxation parameters $\omega = 1.0$ and $\omega = 1.5$ and a different number of pre- and post-smoothing steps, where ν_1/ν_2 means a V-cycle with ν_1-pre and ν_2-post-smoothing steps.

Table 4.3 gives the results for the two-dimensional problem. The choice of $\omega = 1.5$ leads to better results than the normal Gauß–Seidel method. For example, for 90422 unknowns one gets $\rho = 0.31$ instead of $\rho = 0.48$ with one pre- and post-smoothing step. Surprisingly, the number of pre- and post-smoothing steps does not influence the convergence behavior very much. As it can be seen in Figure 4.5, the hierarchy of coarse grids with the strong couplings is very similar to the structure of the model-problems on the unit square.

We notice a different behavior of the method for the three-dimensional problem with linear elements. Table 4.4 shows that this time the chosen smoother as well as the number of smoothing steps play an essential role for the quality of convergence. So, for example in the case of one pre- and post-smoothing step and $n = 29823$, the method provides a convergence of $\rho = 0.26$ for $\omega = 1.5$ instead of $\rho = 0.32$ for $\omega = 1.0$. For two pre- and post-smoothing steps, one even obtains $\rho = 0.07$ for $\omega = 1.5$ and $\rho = 0.18$ for $\omega = 1.0$.

For many problems it is necessary to discretize them on grids, where the mesh width can vary substantially over the domain. One of the main goals of AMG is to provide fast convergence for discretizations of this type. Therefore we look at a discretization in two dimensions on the unit square where the mesh width becomes smaller to the bottom side of the rectangle. An example of such a grid is given in Figure 4.6. Since the variation of mesh width is small locally, the quality of interpolation,

TABLE 4.4
Results for the three-dimensional problem on the sphere with linear elements using Point-Interpolation.

	$\omega = 1.0$			$\omega = 1.5$				
n	1/1	2/1	2/2	1/1	2/1	2/2	c(A)	c(G)
8187	0.27	0.19	0.14	0.26	0.13	0.07	3.44	1.52
20697	0.27	0.20	0.15	0.26	0.13	0.07	3.70	1.50
29823	0.32	0.21	0.18	0.26	0.14	0.07	3.77	1.50

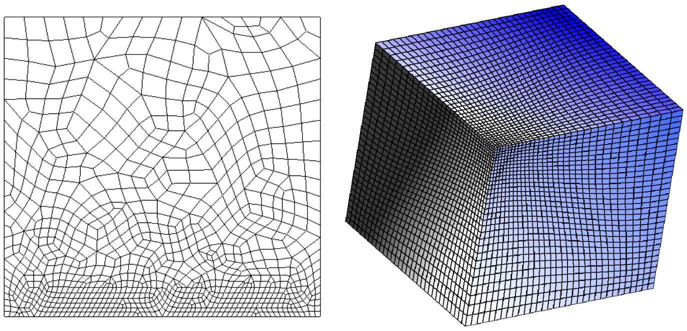

FIGURE 4.6. *Left: Example of a two-dimensional local refined grid. Right: Grid of the three-dimensional problem.*

should be the same as in the previous example. We therefore expect similar results as before. The results from Table 4.5 clearly show the expected behavior. Again, not the number of smoothing steps but the relaxation parameter is of influence for the convergence behavior. So we obtain for example the asymptotic error reduction $\rho = 0.51$ with $\omega = 1.0$ and $\rho = 0.42$ with $\omega = 1.5$ for $n = 152554$.

The grid of the three-dimensional problem on the unit cube is depicted in Figure 4.6 (right). The results for this problem with $n = 89373$ are shown in Table 4.5. The method provides for both smoothers fast convergence of about $\rho \approx 0.3$ for one pre- and post-smoothing step. The best result is reached for two pre- and post-smoothing steps with the SOR-iteration with $\rho = 0.09$.

Finally we show convergence results for the two "real life" geometries shown in Figure 4.7. The discretization with trilinear elements of the geometry depicted on the left leads to a linear system with 89805 unknowns. A standard V-cycle with point standard interpolation and one pre- and post smoothing step of the Gauß–Seidel iteration leads to an average error reduction factor of $\rho = 0.31$. The same results are obtained for our method with SOR-smoothing and $\omega = 1.5$. Varying the number of pre- and post smoothing steps of the Block-SOR smoother improves the convergence substantially. For example in the case of two pre- and post smoothing steps one obtains $\rho = 0.11$ for $\omega = 1.5$ whereas Gauß–Seidel smoothing leads only to a convergence rate of $\rho = 0.23$. The complexities $c(A) = 3.66$ and $c(G) = 1.90$ are similar to the ones in case of the model problem 1.

The second problem discretized with linear elements leads to a linear system with 60592 unknowns. As in the three-dimensional cases with linear elements discussed before, a faster convergence is obtained for SOR-smoothing than for Gauß–Seidel smoothing. For a V-cycle with one pre- and post smoothing step the method converges with $\rho = 0.35$ for Gauß–Seidel smoothing, whereas SOR smoothing leads to $\rho = 0.26$. Also a higher number of smoothing steps improves the results. The convergence rate

TABLE 4.5
Results for the elasticity problems on local refined grids.

	$\omega = 1.0$			$\omega = 1.5$				
two dimensions								
n	1/1	2/1	2/2	1/1	2/1	2/2	c(A)	c(G)
10742	0.41	0.36	0.34	0.30	0.23	0.21	2.94	1.73
41234	0.47	0.43	0.41	0.30	0.31	0.31	2.93	1.69
152554	0.51	0.48	0.47	0.42	0.38	0.38	2.94	1.70
three dimensions								
89373	0.29	0.23	0.19	0.31	0.15	0.09	4.83	1.69

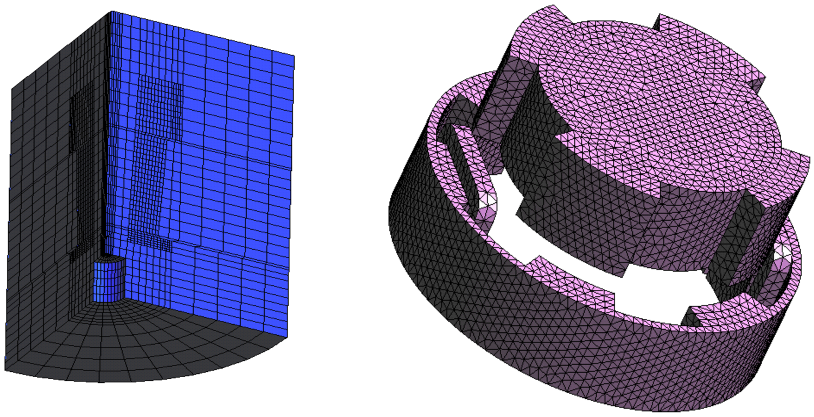

FIGURE 4.7. *Structural part of a motor (left) and a complete motor (right).*

improves to $\rho = 0.19$ for Gauß–Seidel and $\rho = 0.10$ for SOR smoothing with two pre- and post smoothing steps. The operator- and grid-complexities are in the same range as in the previous example with $c(A) = 3.89$ and $c(G) = 1.76$.

5. Concluding remarks. In this paper we presented a generalization of scalar AMG methods to the system case by a point-block approach. We discussed this generalization in more detail for the classic Ruge and Stüben AMG [14] with a newer interpolation formula, the so-called standard interpolation [16]. We were able to prove the exact interpolation of the kernel elements of linear elasticity for the block direct interpolation. Since the exact interpolation of the kernel elements of the continuous operator is important for the speed of convergence of all multigrid algorithms, this result can be seen as a theoretic justification for our approach.

To show the practical relevance of the method, we presented in the second part of the paper some numerical experiments with linear systems stemming from the discretization of linear elasticity problems. First, we tested the method for different mesh widths h of the discretization. Our experiments showed that the convergence is uniformly bounded away from one independent of the mesh width. Also the method is relatively robust with respect to Poisson ratios in the range of $0 \le \nu \le 0.4$, which are in practice the most common cases. Furthermore, the method can also deal with stretched grids and it was successfully applied to adaptive non-uniform grids and complicated geometries.

REFERENCES

[1] D. Braess, *Finite Elemente*, Springer, 1992, ch. 6: Finite Elemente in der Mechanik elastischer Körper, pp. 230–292.

[2] A. Brandt, *Multi-Level Adaptive Technique (MLAT) for Fast Numerical Solution to Boundary Value Problems*, in Proc. of the Third Int. Conf. on Numerical Methods in Fluid Mechanics, Univ. Paris 1972, H. Cabannes and R. Teman, eds., New York, Berlin, Heidelberg, 1973, Springer.

[3] ———, *Multi-Level Adaptive Solutions to Boundary-Value Problems*, Math. Comp., 31 (1977), pp. 333–390.

[4] ———, *Algebraic Multigrid Theory: The Symmetric Case*, in Preliminary Proceedings for the International Multigrid Conference, Copper Mountain, Colorado, April 1983.

[5] A. Brandt, *Multigrid Techniques: 1984 Guide with Applications to Fluid Dynamic*, Tech. Rep. GMD-Studien Nr. 85, 1984.

[6] A. Brandt, *Algebraic Multigrid Theory: The Symmetric Case*, Appl. Math. Comput., 19 (1986), pp. 23–56.

[7] A. Brandt, S. F. McCormick, and J. W. Ruge, *Algebraic Multigrid for Automatic Multigrid Solutions with Application to Geodetic Computations*, tech. rep., Institute for Computational Studies, Fort Collins, Colorado, October 1982.

[8] ———, *Algebraic Multigrid for Sparse Matrix Equations*, in Sparsity and Its Applications, D. J. Evans, ed., Cambridge University Press, 1984.

[9] T. Grauschopf, M. Griebel, and H. Regler, *Additive Multilevel-Preconditioners based on Bilinear Interpolation, Matrix Dependent Geometric Coarsening and Algebraic Multigrid Coarsening for Second Order Elliptic PDEs*, Applied Numerical Mathematics, 23(1) (1997), pp. 63–96. also as SFB-Bericht 342/02/96A Institut für Informatik, TU München, 1996.

[10] M. Griebel, T. Neunhoeffer, and H. Regler, *Algebraic Multigrid Methods for the Solution of the Navier–Stokes Equations in Complicated Domains*, Int. J. Numer. Methods for Heat and Fluid Flow, 26 (1998), pp. 281–301. Also as SFB Bericht 342/1/96A, Institut für Informatik, Technische Universität München.

[11] W. Hackbusch, *Ein iteratives Verfahren zur schnellen Auflösung elliptischer Randwertprobleme*, Tech. Rep. 76-12, Mathematisches Institut, Universität zu Köln, 1976.

[12] ———, *A Fast Numerical Method for Elliptic Boundary Value Problems with Variable Coefficients*, in 2nd GAMM-Conf. numer. Methods Fluid Mech., E. H. Hirschel and W. Geller, eds., Köln, 1977, Deutsche Forschungs- und Versuchsanstalt für Luft- und Raumfahrt, pp. 50–57.

[13] D. Oeltz, *Algebraische Mehrgittermethoden für Systeme partieller Differentialgleichungen*, Diplomarbeit, Institut für Angewandte Mathematik, Universität Bonn, 2001.

[14] J. W. Ruge and K. Stüben, *Efficient Solution of Finite Difference and Finite Element Equations by Algebraic Multigrid*, in Multigrid Methods for Integral and Differntial Equations, D. J. Paddon and H. Holstein, eds., The Institute of Mathematics and its Applications Conference Series, Clarendon Press, 1985.

[15] http://www.sourceforge.net, TOCHNOG, 2001.

[16] U. Trottenberg, C. W. Ossterlee, and A. Schüller, *Multigrid*, Academic Press, San Diego, 2001, ch. Appendix A: An Introduction to Algebraic Multigrid by K. Stüben, pp. 413–532. Also as GMD Report 53.

[17] P. Vaněk, J. Mandel, and M. Brezina, *Algebraic Multigrid based on Smoothed Aggregation for Second and Fourth Order Problems*, Computing, (1996).